JOURNAL OF GEOPHYSICAL RESEARCH, VOL. 113, C11005, doi:10.1029/2008JC004830, 2008

Observed sea ice extent in the Russian Arctic, 1933–2006

Andrew R. Mahoney,[1,2] Roger G. Barry,[1] Vasily Smolyanitsky,[3] and Florence Fetterer[1]

Received 31 March 2008; revised 21 July 2008; accepted 13 August 2008; published 5 November 2008.

[1] We present a time series of sea ice extent in the Russian Arctic based on observational sea ice charts compiled by the Arctic and Antarctic Research Institute (AARI). These charts are perhaps the oldest operational sea ice data in existence and show that sea ice extent in the Russian Arctic has generally decreased since the beginning of the chart series in 1933. This retreat has not been continuous, however. For the Russian Arctic as a whole in summer, there have been two periods of retreat separated by a partial recovery between the mid-1950s and mid-1980s. The AARI charts, combined with air temperature records, suggest that the retreat in recent decades is pan-Arctic and year-round in some regions, whereas the early twentieth century retreat was only observed in summer in the Russian Arctic. The AARI ice charts indicate that a significant transition occurred in the Russian Arctic in the mid-1980s, when its sea ice cover began to retreat along with that of the rest of the Arctic. Summertime sea ice extents derived from the AARI data set agree with those derived from passive microwave, including the Hadley Centre's global sea ice coverage and sea surface temperature (HadISST) data set. The HadISST results do not indicate the 1980s transition or the partial recovery that took place before it. The AARI charts therefore add significantly to our understanding of the variability of Arctic sea ice over the last 8 decades, and we recommend their inclusion in future historical data sets of Arctic sea ice.

Citation: Mahoney, A. R., R. G. Barry, V. Smolyanitsky, and F. Fetterer (2008), Observed sea ice extent in the Russian Arctic, 1933–2006, *J. Geophys. Res.*, *113*, C11005, doi:10.1029/2008JC004830.

1. Introduction

[2] The retreat of Arctic sea ice in recent years has been well documented from satellite observations [e.g., *Parkinson et al.*, 1999; *Stroeve et al.*, 2005], which show an accelerating decline in sea ice extent since 1979. To appreciate the significance of these results, however, it is important to examine sea variability over a longer time period and consider the response of sea ice to climate variability in the past. To do so, we must analyze historic sea ice charts from before the satellite era.

[3] During the second International Polar Year in 1932, the Directorate of the Northern Sea Route was created in Russia to "develop the Northern Sea Route as a regularly operating transport system" [*Barr*, 1991, p. 27]. Shortly afterward, in 1933, the Arctic and Antarctic Research Institute (AARI) began to regularly produce sea ice charts of the Russian Arctic seas based on aerial, ship, and coastal reconnaissance. The AARI ice charts, as we will refer to them, therefore represent the longest operational ice chart record in existence.

[4] Originally hand-drawn, the complete set of AARI ice charts between 1933 and 2006 has recently been digitized. In this study, we analyzed these ice charts to derive up to 74 years of sea ice variability around the Russian Arctic at different times of year. These results allow us to examine the response of the Russian Arctic to early twentieth century warming [*Johannessen et al.*, 2004] and place the recent changes in Arctic sea ice in a longer-term context.

2. Data Set and Methods

2.1. AARI Sea Ice Charts

[5] Data sources used in compiling the charts varied over time, as summarized in Figure 1. Aerial reconnaissance performed by skilled ice observers provided the majority of the data throughout the record. In recent years, airborne and satellite instruments have been increasingly used. Sea ice analysts compile all the available data into charts, which are essentially maps of sea ice conditions important to navigation. Areas of broadly similar composition are labeled with a code, which gives the total sea ice concentration as well as the partial concentrations of different components of the ice cover. Each component is described by its stage of development and the form it takes. Stage of development is given in terms of age and thickness and age category (each category has an associated thickness range). Form is given in terms of floe size and whether or not the ice is landfast. The coding scheme and nomenclature follows World Meteorological Organization (WMO) conventions [*World Meteorological Organization*, 1970].

[1] National Snow and Ice Data Center, University of Colorado, Boulder, Colorado, USA.
[2] Now at Department of Physics, University of Otago, Dunedin, New Zealand.
[3] Arctic and Antarctic Research Institute, St. Petersburg, Russia.

0148-0227/08/2008JC004830$09.00

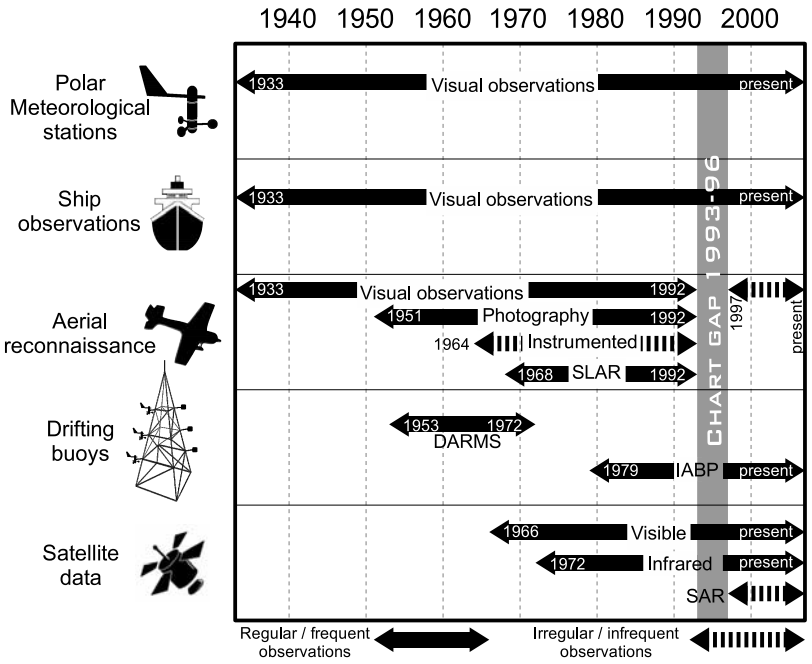

Figure 1. Summary of the different observational methods used to compile the AARI sea ice charts. More details of the different observation platforms and techniques are given in the online data set documentation [*AARI*, 2007].

[6] Observers use a variety of surface attributes to distinguish different developmental stages and forms of sea ice including color; snow patterns; and the form of floe boundaries, cracks, hummocks, and ridges [*Karelin et al.*, 1946; *Arctic Climatology Project*, 2000a]. The WMO age categories are based on the stages of ice development that can be discerned by eye or with visual band data. Topographic features on old ice (ice that has survived a summer's melt season) are generally smoother than on younger ice (WMO subdivides old ice into second-year and multiyear ice. Here we use multiyear to refer to all ice that has survived a summer's melt season). Observers gain skill because observations often support on-ice operations that provide feedback to the operational centers on true ice conditions. Visual observations from reconnaissance flights have, until relatively recently, been the mainstay of operational ice services around the world [*World Meteorological Organization*, 2006], including the Canadian Ice Service [*Meteorological Service of Canada*, 2005] and the U.S. National Ice Center [*National Ice Center*, 2006].

[7] The earliest chart in the AARI data set is from July 1933. Charts were produced every 10 or every 30 days, depending on time of year. Spatial coverage did not extend far into the central Arctic, and the charts were only produced during the summer months in the early part of the series. The period 1993–1996 is missing from the data set. After this gap in chart production, spatial and temporal coverage became more complete as a result of increasing reliance on satellite data, but ice concentration was given in coarser intervals, and multiyear (MY) sea ice concentrations were no longer reported during the summer months.

[8] At AARI, charts were digitized in sea ice grid (SIGRID) format on a 0.25° × 0.25° geographic grid for the domain north of 60°N. These were converted to 12.5-km Equal-Area Scalable Earth Grid (EASE-Grid) at the National Snow and Ice Data Center (NSIDC). In the process, the WMO stage of development classifications encoded in SIGRID were binned into MY, first-year (FY), and new and young age classes. Each EASE-Grid chart file has five separate bands with the concentration of these three classes, as well as total concentration, and a band indicating whether ice is drifting or landfast. Detailed documentation including reconnaissance flight paths, additional references, sample images of chart data, and the EASE-Grid data are available from NSIDC [*AARI*, 2007].

2.2. Calculation of Sea Ice Extent

[9] The gridded ice chart data replicate the original chart coverage (no interpolation was used). Chart coverage varied depending on observations that were available. The EASE-Grid data are therefore spatially discontinuous, so it is not possible to integrate ice concentration over the domain to obtain ice extent (the total area covered by ice at any concentration above a cutoff) or ice area (ice concentration per unit area summed over the area of interest). However, by locating discrete points along the ice edge we were able to calculate the extent of ice in different regions of the Russian Arctic. To do this, we developed an automated algorithm that located the ice edge along meridional transects that follow integer lines of longitude (Figure 2). Because of a lack of sufficient data coverage we only consider the western (Russian) area of the Chukchi Sea. Similarly, the sea ice edge could not be consistently located in the westernmost sector of the Kara Sea, so this is excluded from our analysis.

[10] Along each transect the algorithm attempts to identify three different ice edges as described below.

[11] 1. The landfast ice edge is defined as the northernmost pixel of landfast ice contiguous with the coast (excluding landfast ice around islands).

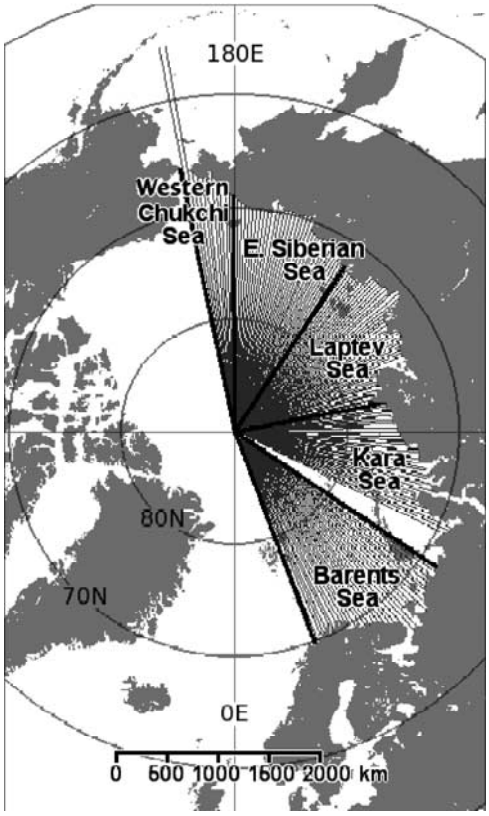

Figure 2. Lines of longitude used to locate the ice edge. The profiles are grouped according to marginal seas. The eastern half of the Chukchi Sea was omitted because of insufficient data coverage. Similarly, the sea ice edge could not be consistently located in the westernmost sector of the Kara Sea. This area is excluded from the analysis.

[12] 2. The drift ice edge is defined as the northernmost transition from <15% to ≥15% total ice concentration. If the ice concentration is ≥15% along the whole transect, the drift ice edge is defined by the landfast ice edge or the coast if no landfast ice is present.

[13] 3. Where MY ice is present along a transect in concentrations greater than 15%, the MY ice edge is defined as the coastline or the transition from <15 to ≥15% in MY ice concentration, whichever is northernmost.

The landfast ice and drift ice edges are illustrated in Figure 3a.

[14] Since this technique does not define a continuous sea ice edge, it cannot represent polynyas or deep embayments. These features lead to multiple intersections of a transect with the ice edge. In general, we take the southernmost of these, which will lead to a small overestimation of ice extent. The dotted circle in Figure 3a highlights an area of a chart that illustrates this. Transects that do not intersect an identifiable ice edge are assigned a null value for ice edge position.

[15] Having defined points along the ice edge according to their longitude and distance from the pole, we calculated the ice extent over 1°-wide sectors of the Arctic Ocean (Figure 3b) and summed these to obtain the ice extent in each marginal sea (see Figure 2 for the boundaries of each sea). Where chart coverage is incomplete, we calculate the mean ice extent from the data available and assume that it is representative of the whole sea.

[16] For each marginal sea, we then calculated the seasonal mean extent by binning the charts into winter, spring, summer, and autumn. Though not consistent with the phenological Arctic summer and winter seasons, for simplicity, we define these four seasons as the 3-month periods beginning with January, April, July, and October, respectively. Extent over the entire Russian Arctic was obtained by summing the mean seasonal extents within each sea. Where one or two seas within the region are missing data for a season, we substitute their 10-year mean centered on the missing data. If mean seasonal extent for more than two seas was missing, mean extent for the entire Russian Arctic was not calculated.

2.3. Ice Extent Calculation Errors

[17] Errors in the ice extent calculations can arise from two sources: inaccurate location of the sea ice edge and sparseness of chart data. Ice edge location errors can in turn be caused by incorrect identification of the edge pixels in the gridded data or by inaccuracies in the charts. To mitigate errors introduced by the edge location algorithm, the ice edges in all 2877 ice charts were inspected manually and corrected where necessary. As a result we estimate the edge to be located within two EASE-Grid pixels or ±25 km, which is the approximate meridional resolution of the SIGRID data. We treat these as uniformly distributed independent errors and so multiply the uncertainty by $\sqrt{N_T}$ when summing N_T transects (where N_T is the total number of edge points used to calculate the seasonal mean) within a sea over a particular season [*Taylor*, 1997].

[18] Inaccuracies in the charts themselves can arise from a combination of observational errors (underestimating or overestimating concentration or misidentifying ice types) and navigation errors. It is difficult to gauge the magnitude of these errors in terms of their effect on the location of the ice edge, but we conservatively estimate that they may result in a ±50-km error in ice edge location (AARI gives 50 km as the possible error in edge location for areas between flight lines. *Polyakov et al.* [2003] cite an accuracy of 2–10 km for similar data from AARI). For an ice edge 1500 km from the pole, the combined edge location errors of ±75 km give a relative error of 5%, which becomes 10% when we square the distance to calculate ice extent. We assume that on the scale of an individual sea, these errors will be constant within a given chart but are otherwise independent and randomly distributed over multiple charts. Hence, the net error in the seasonal mean extent is reduced by a factor of $\sqrt{N_C}$ when averaging over N_C charts (where N_C is the number of charts produced) within a 3-month period [*Taylor*, 1997].

[19] To assess the sensitivity of ice extent calculations to missing chart data, we randomly culled the ice edge data and compared the resulting mean sea ice extent values to the unculled means. We culled spatially by randomly removing edge points from within a given sea and temporally by randomly excluding whole charts from a given season. We culled increasing amounts of the data, performing the comparison a large number of times for each degree of

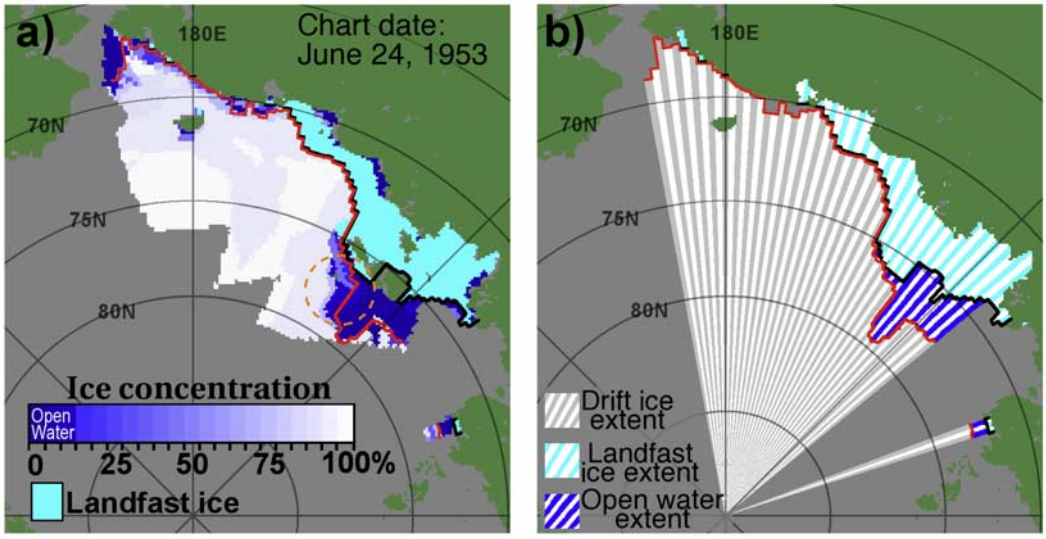

Figure 3. (a) The drift ice edge (red) and landfast ice edge (black) in the eastern Russian Arctic. The landfast ice edge is defined as the northernmost pixel of landfast ice contiguous with the coast. The drift ice edge is defined as the northernmost transition from <15% to ≥15% total ice concentration. If the ice concentration is ≥15% along the whole transect, the drift ice edge is defined by the landfast ice edge or the coast if no landfast ice is present. (b) Drift ice, landfast ice, and open water extents. The dotted circle in Figure 3a highlights an area where, because of an embayment in the ice edge, an area with <15% concentration is included in the sea ice extent. The 1°-wide sectors used to calculate extents are shaded alternately for clarity. The areas of islands are subtracted from all extents.

culling (Figure 4). With only three charts for any given season of a year (Figure 4a) or only 10% of the ice edge defined in a given sea (Figure 4b), the resulting mean ice extent is within 5% of the unculled mean in 95% of the cases. These results demonstrate that accurate seasonal mean ice extents can be calculated within individual seas with relatively little chart coverage. The resulting net error in mean ice extent for a given sea, season, and year therefore depends upon three properties of the ice edge data: f_e, the fraction of the ice edge located within the sea; N_C; and N_T.

[20] These error values and values for f_e, N_C, and N_T are available along with the seasonal mean extent data from NSIDC [*Mahoney*, 2008]. N_C is consistently highest in the

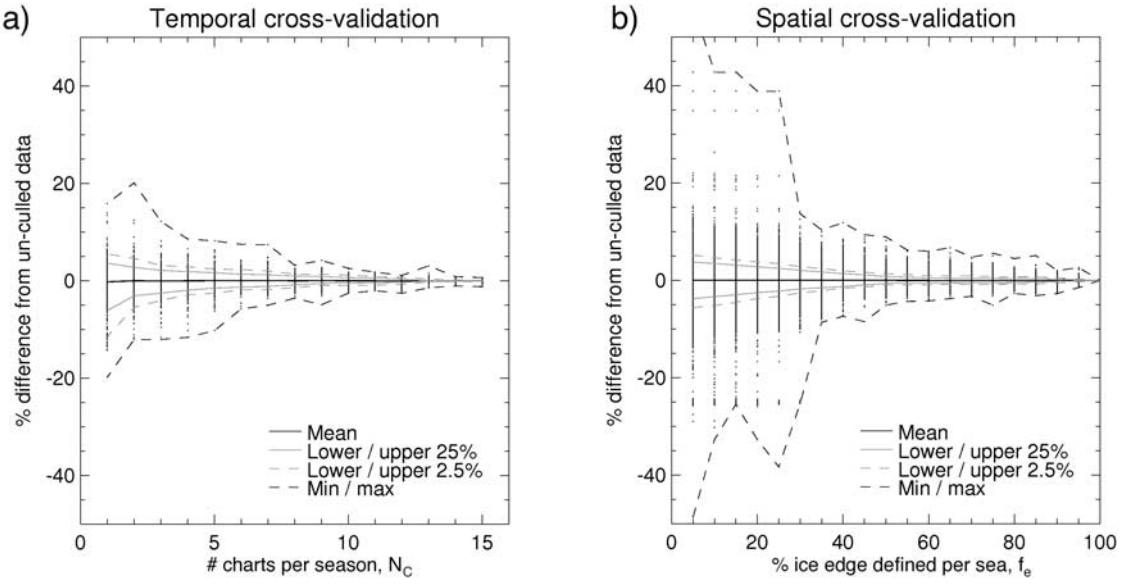

Figure 4. Cross-validation results to test the sensitivity of the seasonal means to (a) missing charts and (b) missing data within a chart. We calculate the distribution of differences resulting from a comparison between values derived from the whole data set and values derived from a randomly culled data set. The test is repeated a large number of times for different fractions of the data set culled.

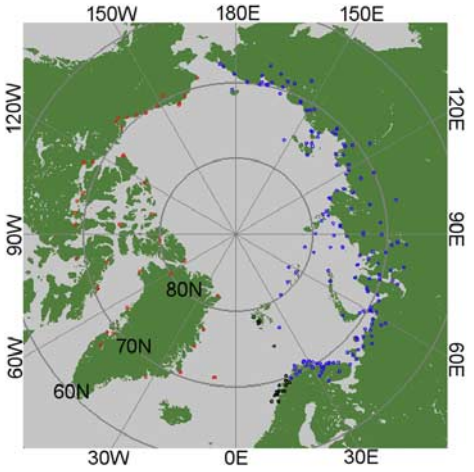

Figure 5. The locations of meteorological stations used in this study. Those in the Russian Arctic and the North American Arctic are show in blue and red, respectively. The stations shown in black were used only in the calculation of Arctic-wide mean values.

summer, with between six and nine charts per season for the large majority of the record. There are fewer charts in the other seasons up until the mid-1970s, after which N_C is more uniform through the year. The coverage of individual charts also varies through the record and by season. Prior to 1945, it is only in summer charts that we were typically able to identify more than 50% of the ice edge within a sea. After this, values of f_e are generally greater than 65%, except for autumn charts, in which f_e is typically between 50 and 70%.

2.4. Meteorological Station Data

[21] Surface air temperature records from three data sets provided a record of climate variability. We used station data from the Integrated Surface Database [*Lott et al.*, 2001], the Arctic Climatology Project Arctic Meteorology and Climate Atlas [*Arctic Climatology Project*, 2000b], and Meteorological Data From the Russian Arctic [*National Snow and Ice Data Center*, 2003]. Combining these data sets, we identified 231 stations above 67°N and within 100 m of sea level that provided data continuously for a minimum period of 30 years. These included 167 stations in the Russian Arctic and 44 stations in the North American Arctic (Figure 5). We calculated monthly means for each station before calculating regional means.

3. Results

[22] Sea ice extent for all four seasons and for each marginal sea is shown with error bars in Figure 6. The error bars represent approximately two standard deviations of the error distributions above and below the mean. We calculated the total sea ice cover extent by summing the drift ice and landfast ice extents (Figure 3b). The blue regions represent a large number of curves overlain on top of each other, with the shade of blue indicating the density of the curves. To generate these curves, we randomly sampled the error at each data point and applied different averaging periods between 5 and 20 years. We then repeated this process a large number of times. This reveals a multi-decadal variability that is relatively insensitive to the smoothing interval or the estimated errors.

[23] Figure 6 shows that sea ice variability in the Russian Arctic during winter and spring is distinctly different from that during summer and autumn. The winter and spring pack ice edge in the eastern Russian Arctic (the Laptev, East Siberian, and western Chukchi seas) lies very close to the landfast ice edge or the coast, and there is little interannual variability in sea ice extent at this time of year. Closer to the Atlantic Ocean, the Kara and Barents seas dominate interannual sea ice variability in wintertime and springtime over the entire Russian Arctic. In the summer and autumn months, by contrast, Figure 6 shows that there is considerable interannual variability in all of the marginal seas. Over the whole record, each of the marginal seas in the Russian Arctic has experienced a general retreat of sea ice. This retreat has not been constant, however, and the smoothed data show multiple periods of advance and retreat.

[24] A valuable and unique aspect of the AARI data set is the long record of MY ice concentrations. The MY ice edge derived here is analogous to the boundary of the perennial ice zone (PIZ) described by *Kwok* [2004]; that is, the PIZ is composed primarily of MY ice. Figure 7 shows the MY ice extent (as defined in section 2.2) together with the estimated errors and the results of smoothing, as in Figure 6. The total extent of the ice cover does not vary much from year to year during winter and spring over most of the Russian sector of the Arctic (Figure 6) because, with the exception of the Barents Sea, sea ice generally covers the entire region. However, the extent of MY ice within the pack does vary considerably from year to year in all seasons, as shown by Figure 7.

[25] As with total sea ice extent, there has been an overall reduction in MY ice extent over the chart record with periods of both advance and retreat. The MY record shows a difference between the eastern and western Russian Arctic in the first half of the record. Until about the early 1980s, MY concentration in the eastern seas tends to be high when that in the western seas is low. Compare, for example, the western Chukchi Sea to the Barents and Kara seas in winter and spring. Beginning in the early 1980s, all seas show a similar downward trend in MY extent for all seasons with the exception of summer (for which no MY ice concentrations were reported after 1992). As a result, the Russian Arctic taken as a whole shows stable or increasing MY ice extent up until the early 1980s, when MY ice extent began declining rapidly. This is in line with other reports of recent declines in MY sea ice [*Maslanik et al.*, 2007; *Nghiem et al.*, 2007].

[26] Figures 6 and 7 show periods of both advance and retreat during the chart record, with transitions being defined by local maxima and minima. The exact timing of each maximum and minimum varies between seas and seasons and also depends upon how the error is sampled and how the data are smoothed (as indicated by the smoothness of the blue regions). However, most of the seas exhibit a local minimum in summertime total sea ice extent around the 1950s–1960s and a local maximum in the 1980s (Figure 6). Up until the 1950s–1960s and after the 1980s, summertime sea ice extent was decreasing around the Russian Arctic. During the intervening period, the retreat of sea ice slowed or reversed. A pattern of alternating trends in extent can also be seen in the MY ice record (Figure 7). In

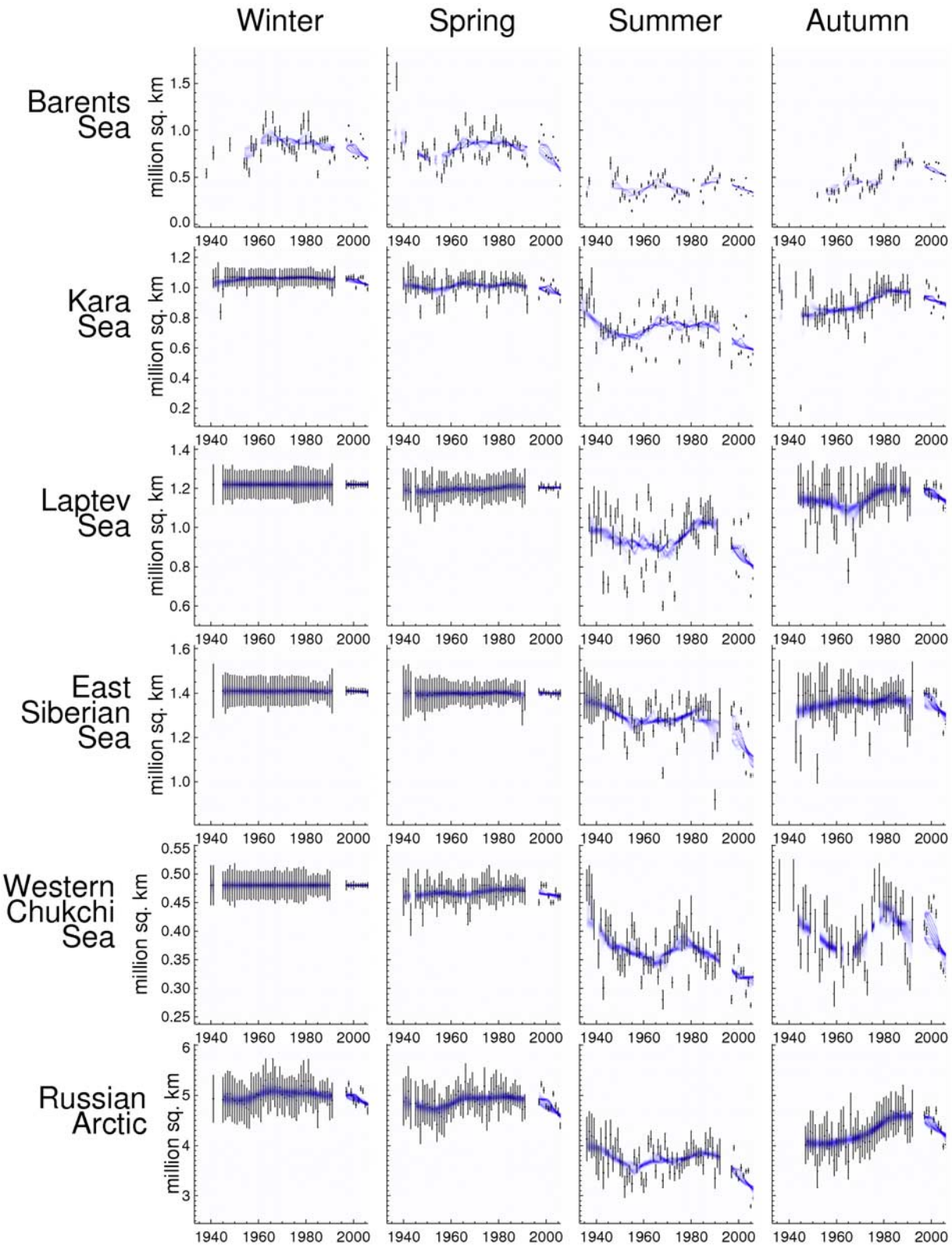

Figure 6. Mean seasonal sea ice extent in each of the Russian marginal seas. The bars show the estimated 95% error margins for each data point. The blue regions show the combined results of smoothing over different intervals with randomly sampled errors. See text for details.

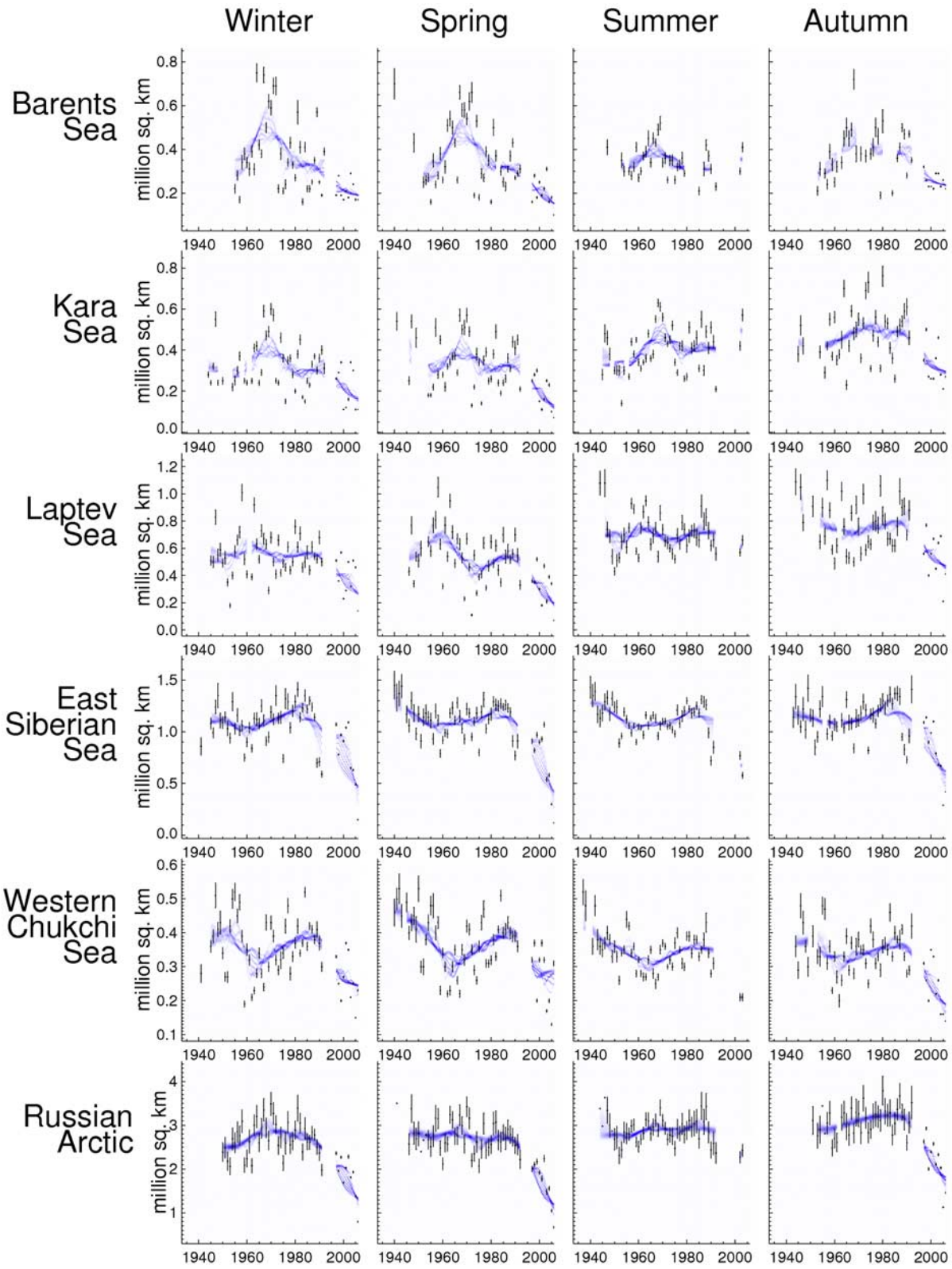

Figure 7. Mean seasonal multiyear sea ice extent in each of the Russian marginal seas. The bars show the estimated 95% error margins for each data point. The blue regions show the combined results of smoothing over different intervals with randomly sampled errors. See text for details.

the eastern seas, these resemble the summertime total sea ice extent variability described above. However, MY ice extent in the Barents and Kara seas appears to have been declining since the late 1960s. This is in agreement with results from a drift-age model presented by *Nghiem et al.* [2007] that suggests a reduction in MY ice since the 1960s.

[27] We can therefore broadly divide the ice chart record into three periods. Period A, extending from the beginning of the record until the mid-1950s, was a period of declining summer sea ice extent over the whole Russian Arctic, though not consistently in every individual sea. Period A is not evident in the winter and spring months and is not as well defined during the autumn partly because of a lack of sea ice charts at this time of year at the beginning of the record. Period B extended from the mid-1950s to the mid-1980s and was a period of generally increasing or stable summer sea ice extent. For the Russian Arctic as a whole, this constituted a partial recovery of the sea ice lost during period A, though this is not the case in all seas. Periods A and B can also be seen in the MY ice record for the overall Russian Arctic (Figure 7), though as mentioned earlier, MY ice extent in the Barents and Kara seas peaked in the 1960s. Period C began in the mid-1980s and continued to the end of the record. It is characterized by a decrease in total and MY sea ice extent in all seas and seasons. In this regard, period C is markedly different from periods A and B.

[28] These results were checked against ice extents derived from two other data sets: passive microwave sea ice concentrations derived using the NASA Team algorithm, 1978–2006 [*Meier et al.*, 2006], and the Hadley Centre's global sea ice coverage and sea surface temperature (HadISST) data set [*UK Meteorological Office*, 2006]. These data sets do not have information on MY sea ice extent, but they are both spatially complete, so we did not have to use the technique described in section 2.2. Instead, we calculated ice extent by summing the areas of grid cells with $\geq$15% concentration within the study region.

[29] Seasonal time series of ice extent from all three data sets (Figure 8) show declining extent for the period since the mid-1980s, though discontinuities in the records lead to edge effects in the smoothed curves, which complicate the comparison. HadISST incorporates passive microwave observations, so we expect broadly similar extents and trends between the HadISST and NASA Team data. The general agreement between AARI charts and other data sets from the mid-1980s on is notable because while the AARI charts incorporate satellite observations (and use them almost exclusively from 1996 on), the AARI ice charts do not incorporate passive microwave data. The agreement within this period also confirms that the AARI data are consistent either side of the 1993–1996 chart gap.

[30] Agreement between the AARI and NASA Team results shown in Figure 8 range from a squared correlation value (R^2) of 0.59 in autumn to one of 0.82 in summer. In autumn, all three data sources differ from the beginning of the passive microwave until the mid-1980s, with the NASA Team showing little trend in extent, AARI charts showing increasing extent, and HadISST showing declining extent. The reasons for these differences are not entirely clear, and an investigation of them is outside the scope of this paper, but listing relevant differences in the data products may point to possible causes.

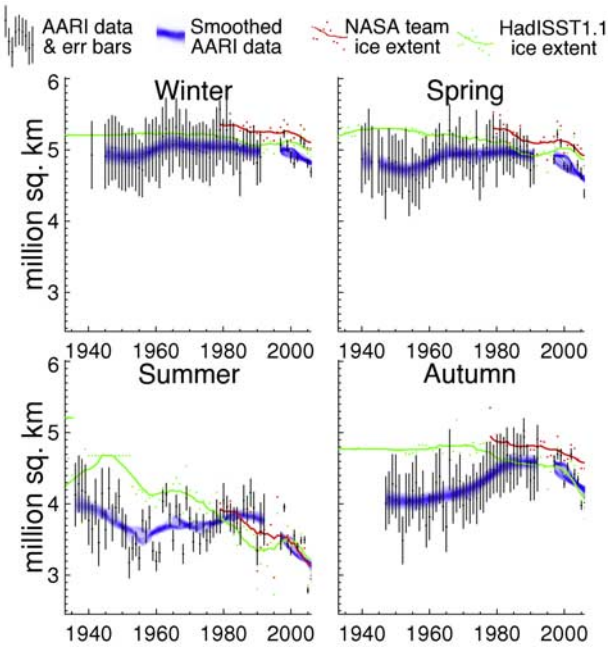

Figure 8. Mean seasonal sea ice extent for the whole Russian Arctic calculated from three sources. The black points with error bars and the blue regions are the same as in the Russian Arctic plots of Figure 6. The red and green points show sea ice extent calculated from passive microwave data and the HadISST data set, respectively. The red and green lines are the 10-year running means of the corresponding data points.

[31] The sources used to compile the HadISST data set are given by *Rayner et al.* [2003]. Up to 1978, HadISST used the Northern Hemisphere Walsh fields [*Walsh and Chapman*, 2001] as its main data source, which in turn relied upon ice charts from a number of different sources to locate the sea ice edge. However, prior to satellite observations, none of these charts provided coverage in the Russian Arctic further east than the Kara Sea [*Kelly*, 1979; *Vinje*, 2001]. Where no sea ice edge data were available, a baseline climatology was used. Such instances are apparent in Figure 8 where the green data points are constant from year to year in the early part of the record. From 1978 through 1986, HadISST used passive microwave data processed with the NASA Team algorithm, adjusted for low summertime ice concentrations using a National Ice Center chart-based climatology. In 1997, the source for the passive microwave data changed to the National Center for Environmental Prediction. These changes are possible sources of discontinuities in the HadISST record.

[32] The discrepancy between the AARI record and the other data sets in the early part of the passive microwave record is difficult to reconcile and consequently reduces our certainty in the earlier AARI record. However, the discrepancy coincides with poor autumn coverage in the Barents and Kara seas, which is where the majority of the difference occurs. There is therefore reason to believe that the difference may be limited to autumn months in the early 1980s in the western Russian Arctic. This is supported by the higher correlations between AARI and passive microwave results in the other seasons.

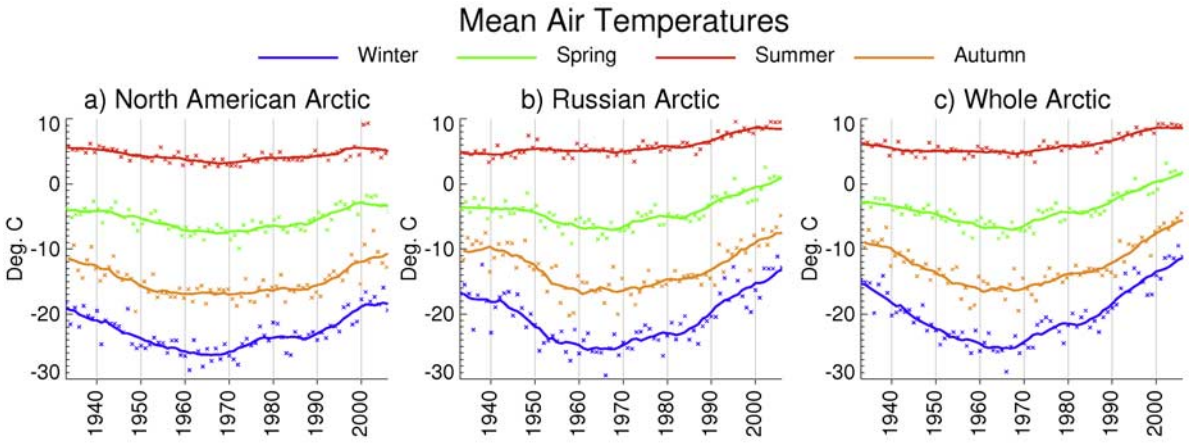

Figure 9. Seasonal surface air temperature variability in (a) the North American Arctic, (b) the Russian Arctic, and (c) the whole Arctic. Calculated from station data described in section 2.4.

[33] Comparisons between sea ice data from charts and from passive microwave observations usually show that passive microwave observations detect less ice than do the more manual methods of interpreting many sources of information to create charts [e.g., *Partington et al.*, 2003]. Therefore, it is somewhat surprising that the AARI charts show a slightly lower ice extent than do the passive microwave data, and we do not have an explanation at this stage.

[34] Prior to the passive microwave record, the AARI and HadISST results diverge. During summer, when there is the best agreement between AARI and HadISST during the passive microwave record, the two data sets both show an overall decline in sea ice extent since the beginning of the AARI record. However, the climatological values used by HadISST prior to the 1950s show significantly more ice than the AARI charts. Also, the HadISST data do not indicate any recovery of ice extent between the 1950s and 1980s. Results for marginal seas (not shown) are similar.

4. Discussion

[35] Figures 6 and 7 indicate an overall reduction in sea ice extent within the Russian Arctic since 1933. This retreat has not been constant: over the region as a whole during summer, there have been two periods of retreat (periods A and C) separated by a period of partial recovery (period B). These periods and their timing agree well with the three periods of sea ice variability identified by *Zakharov* [1997]. For each individual sea, the summer sea ice extent shown in Figure 6 closely matches the August sea ice extent presented by *Polyakov et al.* [2003], though they did not identify the three periods of variability.

[36] Alternating multidecadal trends are evident in other Arctic time series such as mean surface air temperature [*Johannessen et al.*, 2004] and intermediate Atlantic water temperature [*Polyakov et al.*, 2004]. These time series indicate a period of warming in the early twentieth century, followed by a period of cooling that is followed by a second period of warming in recent decades. Qualitatively, therefore, these trends coincide with those in Russian sea ice extent. However, mean Arctic surface air temperatures and intermediate Atlantic water temperatures both transitioned from warming to cooling in the late 1930s. This means that Russian sea ice extent was still decreasing (period A) while the Arctic as a whole was cooling.

[37] Examining temperatures in the Russian Arctic separately (Figure 9), we see that summer air temperatures in the Russian Arctic were still increasing while elsewhere and in other seasons they were decreasing at the end of the early twentieth century warm period [*Johannessen et al.*, 2004]. Because of the close link between sea ice and air temperature [e.g., *Polyakov et al.*, 2003; *Johannessen et al.*, 2004; *Serreze et al.*, 2008], we therefore propose that the variations in sea ice in the Russian Arctic were not synchronized with those in the rest of the Arctic at this time.

[38] On the basis of data in Figures 6 and 7, the proportion of MY ice within the ice cover has decreased along with the overall MY ice extent during the period of record. Figure 7 shows that MY ice extent began to decrease rapidly in the mid-1980s for most seasons and regions. This decline begins a few years earlier than the tipping point proposed by *Lindsay and Zhang* [2005, p. 4893], who suggest that a change in atmospheric circulation led to a "flushing of some of the older, thicker, ice out of the basin" in 1988. The "flushing" event is described as a response of sea ice to the Arctic Oscillation [*Rigor et al.*, 2002], though overall there is no correlation between our results and the Arctic Oscillation index.

[39] The reduction in MY ice extent is significant. Its greater thickness means that MY ice is a more efficient insulator of ocean heat and contributes more freshwater when it melts than FY ice. MY ice also requires more energy to melt, which means that it acts as a resilient core to the overall sea ice cover during summer and limits the extent to which the sea ice cover can retreat. The loss of MY ice may therefore accelerate the rate of retreat of the overall Arctic sea ice cover.

5. Conclusions

[40] The AARI sea ice charts provide the most detailed record of ice conditions in the Russian Arctic for the period before satellite observations became routine. By locating

positions along the ice edge, we have calculated regional and seasonal time series of Russian Arctic sea ice extent as far back as 1933. Our results show that sea ice was most extensive at the start of the record and has since experienced two periods of decline, evident in the summer means. The first of these was during the 1930s–1950s (period A), and the second began in the mid-1980s and is still ongoing (period C).

[41] Examining seasonal sea ice extent in the different marginal seas of the Russian Arctic, we find qualitative differences that distinguish the two periods of retreat. During period A, the retreat is evident in the overall Russian Arctic but not in every individual sea. During period C, however, the retreat can be seen in all seas. The wintertime retreat in the Barents and Kara seas is only evident during period C. The surface air temperature record also reveals a difference between the two periods of retreat and suggests that the period A retreat may have been confined to the Russian Arctic, whereas satellite records show that the current period of retreat is occurring Arctic-wide [*Meier et al.*, 2007].

[42] Periods A and B are not evident in the HadISST data, which show a more continual decline in summertime Russian sea ice during the twentieth century. Although we have reason to question the quality of the early AARI data in autumn months, the good correlation with passive microwave results gives us confidence in the summertime AARI ice extents. The HadISST data therefore miss a potentially important transition that occurred in the 1980s, when the Arctic sea ice retreat became a basin-wide and year-round phenomenon. *Rayner et al.* [2003] acknowledge that the AARI charts, which were not available in digital form at the time, were not incorporated into the HadISST data set, but we strongly encourage their assimilation in future updates.

[43] Using HadISST data, *Meier et al.* [2007] compared the linear trend in September sea ice extent during 1953–2005 to that during 1979–2005 and concluded that the retreat of Arctic sea ice accelerated slightly in recent decades. Had the AARI charts been available to Meier et al. they may have instead concluded that a more significant change had occurred since our results show a transition from advance to retreat during this time.

[44] **Acknowledgments.** This work was funded through the National Aeronautics and Space Administration (NASA award NNG04GH03G). We are also grateful to the staff at AARI who were instrumental in checking, compiling, and digitizing the sea ice charts, in particular to Victor Borodachev (supervisor of ice charting group in 1970–1990s), Vasily Shilnikov, Vasily Belov, Tomash Petrovsky, and Irina Revko. We also thank Andrew Slater for valuable discussions regarding data and error analysis. The AARI data set is maintained and distributed by NSIDC with support from the NOAA-NESDIS National Geophysical Data Center.

References

Arctic and Antarctic Research Institute (AARI) (2007), Sea Ice Charts of the Russian Arctic in Gridded Format, 1933–2006, http://nsidc.org/data/g02176.html, Natl. Snow and Ice Data Cent., Boulder, Colo.

Arctic Climatology Project (2000a), *Environmental Working Group Joint U.S.-Russian Arctic Sea Ice Atlas* [CD-ROM], Natl. Snow and Ice Data Cent., Boulder, Colo.

Arctic Climatology Project (2000b), *Environmental Working Group Arctic Meteorology and Climate Atlas* [CD-ROM], Natl. Snow and Ice Data Cent., Boulder, Colo.

Barr, W. (1991), The Arctic Ocean in Russian history to 1945, in *The Soviet Maritime Arctic*, edited by L. W. Brigham, pp. 11–32, Belhaven, London.

Johannessen, O. M., et al. (2004), Arctic climate change: Observed and modelled temperature and sea-ice variability, *Tellus, Ser. A*, *56*, 328–341.

Karelin, D. B., N. A. Volkov, V. V. Shadrinksy, and P. A. Gordiyenko (1946), *Ledovaya Aviatsionnaya Razvedka (Airborne Ice Reconnaissance)*, Izdatel'stvo Glavsevmorputi, Moscow.

Kelly, P. M. (1979), An Arctic sea ice data set, 1901–1956, in *Glaciological Data*, *Rep. GD-5*, pp. 101–104, World Data Cent. for Glaciol., Boulder, Colo.

Kwok, R. (2004), Annual cycles of multiyear sea ice coverage of the Arctic Ocean: 1999–2003, *J. Geophys. Res.*, *109*, C11004, doi:10.1029/2003JC002238.

Lindsay, R. W., and J. Zhang (2005), The thinning of Arctic sea ice, 1988–2003: Have we passed a tipping point?, *J. Clim.*, *18*, 4879–4894, doi:10.1175/JCLI3587.1.

Lott, N. R., R. Baldwin, and P. D. Jones (2001), The FCC integrated surface hourly database: A new resource of global climate data, *Tech. Rep. 2001-01*, 42 pp., National Clim. Data Cent., Asheville, N. C.

Mahoney, A. (2008), Sea Ice Edge Location and Extent in the Russian Arctic, 1933–2006, http://nsidc.org/data/g02182.html, Natl. Snow and Ice Data Cent., Boulder, Colo.

Maslanik, J. A., C. Fowler, J. Stroeve, S. Drobot, J. Zwally, D. Yi, and W. Emery (2007), A younger, thinner Arctic ice cover: Increased potential for rapid, extensive sea-ice loss, *Geophys. Res. Lett.*, *34*, L24501, doi:10.1029/2007GL032043.

Meier, W., F. Fetterer, K. Knowles, M. Savoie, and M. J. Brodzik (2006), Sea Ice Concentrations From Nimbus-7 SMMR and DMSP SSM/I Passive Microwave Data, 1979–2006, http://nsidc.org/data/nsidc-0051.html, Natl. Snow and Ice Data Cent., Boulder, Colo.

Meier, W. N., J. Stroeve, and F. Fetterer (2007), Whither Arctic sea ice? A clear signal of decline regionally, seasonally and extending beyond the satellite record, *Ann. Glaciol.*, *46*, 428–434, doi:10.3189/172756407782871170.

Meteorological Service of Canada (2005), MANICE: Manual of standard procedures for observing and reporting ice conditions, 9th ed., Environ. Can., Ottawa.

National Ice Center (2006), National Ice Center Arctic Sea Ice Charts and Climatologies in Gridded Format, http://nsidc.org/data/g02172.html, Natl. Snow and Ice Data Cent., Boulder, Colo.

National Snow and Ice Data Center (2003), Meteorological Data From the Russian Arctic, 1961–2000, http://nsidc.org/data/g02141.html, Natl. Snow and Ice Data Cent., Boulder, Colo.

Nghiem, S. V., I. G. Rigor, D. K. Perovich, P. Clemente-Colón, J. W. Weatherly, and G. Neumann (2007), Rapid reduction of Arctic perennial sea ice, *Geophys. Res. Lett.*, *34*, L19504, doi:10.1029/2007GL031138.

Parkinson, C. L., D. J. Cavalieri, P. Gloersen, H. J. Zwally, and J. C. Comiso (1999), Arctic sea ice extents, areas, and trends, 1978–1996, *J. Geophys. Res.*, *104*, 20,837–20,856, doi:10.1029/1999JC900082.

Partington, K., T. Flynn, D. Lamb, C. Bertoia, and K. Dedrick (2003), Late twentieth century Northern Hemisphere sea-ice record from U.S. National Ice Center ice charts, *J. Geophys. Res.*, *108*(C11), 3343, doi:10.1029/2002JC001623.

Polyakov, I. V., G. V. Alekseev, R. V. Bekryaev, U. S. Bhatt, R. L. Colony, M. A. Johnson, V. Karlin, D. Walsh, and A. V. Yulin (2003), Long-term ice variability in Arctic marginal seas, *J. Clim.*, *16*, 2078–2085, doi:10.1175/1520-0442(2003)016<2078:LIVIAM>2.0.CO;2.

Polyakov, I. V., G. V. Alekseev, L. A. Timokhov, U. S. Bhatt, R. L. Colony, H. L. Simmons, D. Walsh, J. E. Walsh, and V. F. Zakharov (2004), Variability of the intermediate Atlantic water of the Arctic Ocean over the last 100 years, *J. Clim.*, *17*, 4485–4497, doi:10.1175/JCLI-3224.1.

Rayner, N. A., D. E. Parker, E. B. Horton, C. K. Folland, L. V. Alexander, D. P. Rowell, E. C. Kent, and A. Kaplan (2003), Global analyses of sea surface temperature, sea ice, and night marine air temperature since the late nineteenth century, *J. Geophys. Res.*, *108*(D14), 4407, doi:10.1029/2002JD002670.

Rigor, I. G., J. M. Wallace, and R. L. Colony (2002), Response of sea ice to the Arctic Oscillation, *J. Clim.*, *15*, 2648–2663, doi:10.1175/1520-0442(2002)015<2648:ROSITT>2.0.CO;2.

Serreze, M. C., A. P. Barrett, J. C. Stroeve, D. N. Kindig, and M. M. Holland (2008), The emergence of surface-based Arctic amplification, *Cryosphere Discuss.*, *2*, 601–622.

Stroeve, J. C., M. C. Serreze, F. Fetterer, T. Arbetter, W. Meier, J. Maslanik, and K. Knowles (2005), Tracking the Arctic's shrinking ice cover: Another extreme September minimum in 2004, *Geophys. Res. Lett.*, *32*, L04501, doi:10.1029/2004GL021810.

Taylor, J. (1997), *Introduction to Error Analysis: The Study of Uncertainties in Physical Measurements*, 2nd ed., Univ. Sci. Books, New York.

UK Meteorological Office (2006), HadISST 1.1—Global Sea Ice Coverage and Sea Surface Temperature Data (1870–Present), 1933–2006, http:/badc.nerc.ac.uk/data/hadisst, British Atmos. Data Cent., Rutherford Appleton Lab., Didcot, U. K.

Vinje, T. (2001), Anomalies and trends of sea-ice extent and atmospheric circulation in the Nordic seas during the period 1864–1998, *J. Clim.*, *14*, 255–267, doi:10.1175/1520-0442(2001)014<0255:AATOSI>2.0.CO;2.

Walsh, J. E., and W. L. Chapman (2001), 20th-century sea-ice variations from observational data, *Ann. Glaciol.*, *33*, 444–448, doi:10.3189/172756401781818671.

World Meteorological Organization (1970), *WMO Sea-Ice Nomenclature: Terminology, Codes and Illustrated Glossary*, *WMO Publ.*, vol. 259, 147 pp., Secr. of the World Meteorol. Organ., Geneva, Switzerland.

World Meteorological Organization (2006), *Sea-Ice Information Services in the World*, *WMO Publ.*, vol. 574, 88 pp., Secr. of the World Meteorol. Organ., Geneva, Switzerland.

Zakharov, V. F. (1997), Sea ice in the climate system, *Tech. Doc. 782*, 80 pp., Arctic Clim. Syst. Study, World Clim. Res. Programme, World Meteorol. Organ., Geneva, Switzerland.

R. G. Barry and F. Fetterer, National Snow and Ice Data Center, University of Colorado, UCB 449, Boulder, CO 80309, USA.

A. R. Mahoney, Department of Physics, University of Otago, P. O. Box 56, Dunedin, New Zealand. (mahoney@physics.otago.ac.nz)

V. Smolyanitsky, Arctic and Antarctic Research Institute, 8 Bering Street, St. Petersburg, 199397, Russia.